Research Paper

PAIN®

Striatal opioid receptor availability is related to acute and chronic pain perception in arthritis: does opioid adaptation increase resilience to chronic pain?

Christopher A. Brown[a,f,*], Julian Matthews[b], Michael Fairclough[b], Adam McMahon[b], Elizabeth Barnett[b], Ali Al-Kaysi[c], Wael El-Deredy[d,e], Anthony K.P. Jones[f]

Abstract

The experience of pain in humans is modulated by endogenous opioids, but it is largely unknown how the opioid system adapts to chronic pain states. Animal models of chronic pain point to upregulation of opioid receptors (OpR) in the brain, with unknown functional significance. We sought evidence for a similar relationship between chronic pain and OpR availability in humans. Using positron emission tomography and the radiotracer ^{11}C-diprenorphine, patients with arthritis pain (n = 17) and healthy controls (n = 9) underwent whole-brain positron emission tomography scanning to calculate parametric maps of OpR availability. Consistent with the upregulation hypothesis, within the arthritis group, greater OpR availability was found in the striatum (including the caudate) of patients reporting higher levels of recent chronic pain, as well as regions of interest in the descending opioidergic pathway including the anterior cingulate cortex, thalamus, and periaqueductal gray. The functional significance of striatal changes were clarified with respect to acute pain thresholds: data across patients and controls revealed that striatal OpR availability was related to reduced pain perception. These findings are consistent with the view that chronic pain may upregulate OpR availability to dampen pain. Finally, patients with arthritis pain, compared with healthy controls, had overall less OpR availability within the striatum specifically, consistent with the greater endogenous opioid binding that would be expected in chronic pain states. Our observational evidence points to the need for further studies to establish the causal relationship between chronic pain states and OpR adaptation.

Keywords: Pain, Arthritis, PET, Opioid, Striatum

1. Introduction

Chronic pain is frequently reported by patients with arthritis.[58] However, there is no correlation between pain and structural joint damage in osteoarthritis (OA).[5] The basis of variability between pathophysiology and pain outcomes is unknown. One possibility is natural variability in pain regulation within the central nervous system.

The ascending spinothalamic pathways that mediate nociception terminate in multiple thalamic nuclei and cortical brain regions.[20] Cortical sites modulate nociception partly by projecting to the basal ganglia including the striatum, which also receives afferent nociceptive inputs from the spinal cord through the globus pallidus.[6] Striatal nuclei, including the caudate, putamen, and nucleus accumbens, are the most densely populated regions for opioid receptors (OpRs) in the brain[4,14,34] and are thought to be important for opioid-mediated endogenous analgesia.[12,21] The possibility of opioid mechanisms being involved in determining individual differences in pain states has been a key topic of recent research,[28,41,60] but the functional consequences of chronic pain on OpR physiology are largely unknown.

It has long been known that prolonged nociception results in the release of endogenous opioid peptides and subsequent agonism of OpRs in the central nervous system.[19] However, a relatively unexplored hypothesis is that chronic pain could potentially adjust OpR physiology to provide more efficient dampening of the pain response as part of a homeostatic control mechanism. There is evidence from animal studies that delta and kappa OpRs, found in the brain and spinal cord,[8,11] can be upregulated in response to mu-OpR agonism,[56] thereby increasing the antinociceptive potency of delta-OpR agonists.[38,44] Animal models of chronic inflammatory pain have shown an increase in cell membrane expression of delta-OpRs both postsynaptically[9] and presynaptically[22] in the dorsal spinal

Sponsorships or competing interests that may be relevant to content are disclosed at the end of this article.

[a] CamPAIN Group, Division of Anaesthesia, School of Clinical Medicine, University of Cambridge, Cambridge, United Kingdom, [b] Wolfson Molecular Imaging Centre, University of Manchester, Manchester, United Kingdom, [c] Department of Anaesthesia, Southport and Ormskirk Hospitals, Southport, Merseyside, United Kingdom, [d] School of Psychological Sciences, University of Manchester, Manchester, United Kingdom, [e] Department of Civil Biomedical Engineering, University of Valparaiso, Valparaiso, Chile, [f] Human Pain Research Group, Institute of Brain, Behaviour and Mental Health, University of Manchester, Salford, United Kingdom

**Corresponding author. Address: CamPain Group, Division of Anaesthesia, University of Cambridge, Box 93, Addenbrooke's Hospital, Cambridge CB2 0QQ, United Kingdom. Tel: 01223 256995; fax: 01223 217 887. E-mail address: cb802@cam.ac.uk (C. A. Brown).*

Supplemental digital content is available for this article. Direct URL citations appear in the printed text and are provided in the HTML and PDF versions of this article on the journal's Web site (www.painjournalonline.com).

PAIN 156 (2015) 2267–2275

http://dx.doi.org/10.1097/j.pain.0000000000000299

cord ipsilateral to the site of injury. Stimulus-evoked translocation of delta-OpRs to neuronal plasma membranes may have evolved as part of a homeostatic mechanism to maintain control of nociceptive transmission.[7] However, evidence for such a mechanism in humans is lacking.

Positron emission tomography (PET) receptor–binding studies enable assessment of the endogenous opioid system in humans through radiotracers that bind to OpRs, such as carbon-11-labelled diprenorphine ([^{11}C]-DPN), an antagonist that binds equally well to mu-, delta-, and kappa-OpRs.[31,33] Here, we measured OpR availability in patients with arthritis and healthy controls with [^{11}C]-DPN PET imaging to identify relationships between OpR availability and the level of perceived acute and chronic pain. Our analysis revealed associations between the striatum and the perception of both acute and chronic pain. We interpret our findings in relation to the hypothesis, supported by the aforementioned evidence from the animal literature, of adaptive upregulation of OpR-binding sites in chronic pain states.

2. Materials and methods

The research study was approved by Stockport NHS Research Ethics Committee (Reference 09/H1012/44) and permission was granted by ARSAC (radiation protection agency).

2.1. Participants

Seventeen patients (12 females) and nine healthy control participants (3 females) were recruited into the study. All participants gave written informed consent. The characteristics of the participants are shown in **Table 1**. Patients were recruited from primary and secondary care in Greater Manchester, whereas healthy control participants were recruited from an existing database of research volunteers and from primary care in Greater Manchester. Fifteen participants had a diagnosis of OA, whereas 2 had a diagnosis of rheumatoid arthritis (RA). All patients had experienced chronic pain for at least the past 3 months. Patients with OA and RA fulfilled the American College of Rheumatology (ACR) criteria for the diagnosis of OA[3] and RA.[1] No control participants were experiencing any chronic pain or other recurrent health problems. Exclusion criteria for both groups included age of <35 years and medical records showing a history of neurological disorder, morbid psychiatric disorder (including major depression and anxiety-related disorders confirmed by a psychiatrist), organ failure, or cardiovascular disease. It was expected that patients would be recruited with subclinical levels of anxiety and depression that are normal for chronic pain populations.

Any patients taking opioid analgesic medication, of which there were 2, were asked to withdraw before scanning. The timing of this withdrawal was determined on a case-by-case basis, but was started no more than 2 weeks prior, and completed not later than 2 days prior, to each scanning session. Any paracetamol or non-steroidal anti-inflammatory drugs (NSAIDs) were withdrawn at least 24 hrs before scanning.

2.2. MRI data acquisition and preprocessing

A T_1-weighted MRI brain scan was acquired for the purpose of excluding structural abnormality, coregistration, and spatial normalization of PET images (see Supplementary Methods, available online as Supplemental Digital Content at http://links.lww.com/PAIN/A159). MRIs were segmented into white matter, gray matter, and cerebrospinal fluid using Statistical Parametric Mapping (SPM8; Wellcome Department of Imaging Neuroscience, Institute of Neurology, UCL, London, United Kingdom) running on MATLAB version 7.10 (The Mathworks Inc, Natick, MA).

2.3. Questionnaire assessments

Patients (but not healthy controls) completed an assessment of clinical pain as experienced over the last week, before PET scanning. Clinical pain was measured using the short-form McGill Pain Questionnaire,[42] which has subscales for sensory and affective pain.

2.4. Positron emission tomography scans

A cannula was inserted into a radial artery of the nondominant forearm after a satisfactory modified Allen's test and local anaesthesia, for sampling of arterial blood during the scan. An intravenous cannula was inserted into the dominant forearm for radiotracer injection.

Patients were scanned using a Siemens/CTI High Resolution Research Tomograph (HRRT; CTI/Siemens Molecular Imaging, Knoxville, TN[35]) PET scanner at the Wolfson Molecular Imaging Centre, capable of 2.5 mm resolution. Participants were positioned supine with their transaxial planes parallel to the line intersecting anterior and posterior commissure (AC–PC line). Head position was measured and equated as best as possible in both PET sessions. Head movement during scanning was discouraged by applying gentle pressure to the nasion by means of a padded attachment to the head holder. Patients wore a customized neoprene cap with a reflective tool attached to the vertex that was used to continuously assess head motion using a Polaris Vicra infrared motion detector (Northern Digital, ON, Canada). Before further scanning, a 6-minute transmission scan was performed for attenuation correction, facilitated by a ^{137}Cs transmission point source.[36]

Regional cerebral blood flow (rCBF) was measured to allow for assessment of the relationship of [^{11}C]-DPN binding results to rCBF. After the transmission scan and immediately before the [^{11}C]-DPN scan, 510 to 645 MBq (target dose: 600 MBq) of

Table 1

Group characteristics.

	Total, n	Females, n	Age, y	Weight, kg	DPN dose injected, MBq	H_2O dose injected, MBq	Head motion	Intrascan pain ratings	Thermal pain threshold, W·cm^{-2}
Arthritis patients	17	12	57.5 (12.1)	83.1 (21.0)	490.0 (62.3)	606.7 (22.3)	3.6 (3.3)	2.5 (2.0)	3.9 (1.5)
Healthy controls	9	3	45.4 (7.5)	78.8 (16.2)	505.0 (33.0)	583.4 (30.7)	1.6 (1.8)	1.5 (1.4)	4.0 (1.9)
Independent-sample *t* test *P* statistic		0.08	*0.004*	0.59	0.26	0.07	0.1456*	0.18	0.76

Values are expressed as means (with standard deviation). Equal variances not assumed. All test are parametric *t* tests except for * indicating non-parametric Wilcoxon rank sum test. Italicized values indicate a statistically significant group effect.
DPN, diprenorphine.

^{15}O-labelled water ($H_2{}^{15}O$) was administered, using an automatic radio water generator (HIDEX Inc, Turku, Finland) (see Supplementary Methods, available online as Supplemental Digital Content at http://links.lww.com/PAIN/A159). This was followed by an intravenous smooth bolus subpharmacological tracer dose of [^{11}C]-DPN injected over 20 seconds, followed by a 20-second saline flush. [^{11}C]-DPN was initially synthesized in situ at the Wolfson Molecular Imaging Centre using the methylation method.[18] Characteristics of [^{11}C]-DPN doses are shown in Supplementary Table 1 (available online as Supplemental Digital Content at http://links.lww.com/PAIN/A159). A 90-minute continuous acquisition in list mode followed injection (see Supplementary Methods, available online as Supplemental Digital Content at http://links.lww.com/PAIN/A159).

For both the [^{11}C]-DPN and $H_2{}^{15}O$ scans, continuous measurements of the radioactivity in arterial blood were conducted, and further intermittent discrete arterial blood sampling took place for cross-calibration and to determine the partition of blood radioactivity between plasma and whole blood (erythrocytes) (see Supplementary Methods. available online as Supplemental Digital Content at http://links.lww.com/PAIN/A159).

2.5. Derivation of arterial input function

The input function of parent [^{11}C]-DPN in arterial blood plasma was derived as follows. To obtain the time-course of whole-blood radioactivity over time, the continuous blood data from the first 10 minutes of the [^{11}C]-DPN scan was firstly calibrated against radioactivity measured in discrete blood samples (using a well counter) at corresponding time points. This initial time-course was then spliced with an interpolation of the discrete blood radioactivity data over the remainder of the scan to obtain the full time-course. From the discrete blood samples, the plasma-over-blood ratio was calculated and linearly fitted. Using the radio-HPLC (high performance liquid chromatography) data, the percentage of radioactivity attributed to the parent radiotracer in plasma was fitted as an exponential function in which time 0 was restricted to unity. Input functions were then derived by multiplying (1) the time-course of radioactivity in whole blood, (2) the linear function describing the plasma-over-blood ratio over time, and (3) the exponential function describing the parent fraction in plasma over time.

2.6. [^{11}C]-DPN and $H_2{}^{15}O$ PET image reconstruction

Positron emission tomography images were reconstructed to a $256 \times 256 \times 207$ matrix (isotropic voxel size of 1.21875 mm^3) using an iterative Ordinary Poisson Ordered Subset Expectation Maximization algorithm (OP-OSEM; 12 iterations). The reconstruction was performed using the HRRT user community software with the default resolution kernel.[13] After reconstruction, the dynamic images were trimmed, calibrated, and stored as Analyze 7.5 formatted images. The calibration factor was determined using a uniform head-sized phantom, which is scanned periodically (~every 2 weeks).

2.7. Derivation of ^{11}C-DPN volume of distribution and $K1_{DPN}$

Parametric images of the [^{11}C]-DPN volume of distribution (VD_{DPN}) and the [^{11}C]-DPN rate of uptake from blood to tissue ($K1_{DPN}$) were calculated using spectral analysis[55] and implemented using the nonnegative least squares algorithm (conventional spectral analysis[15]). Inputs to this analysis were the dynamic PET images and the arterial input function, both uncorrected for decay of ^{11}C. The fast frequency boundary was set to 0.02 s$-$1 and the slow frequency boundary to 0.0008 s$-$1. The slow frequency boundary was informed by 2 considerations: (1) the slowest possible kinetics of [^{11}C]-DPN, which is limited by the physical decay constant of the isotope (0.0005663 s$-$1), deriving from the half-life of ^{11}C (20.4 minutes); (2) data evaluating the image quality, reproducibility, and reliability of [^{11}C]-DPN VD images across a range of slow frequency boundaries, which identified 0.0008 s$-$1 as being superior to lower cutoffs that were closer to the decay constant of ^{11}C.[27] The spectra were spaced logarithmically and the magnitude was normalised so that the weighted columns summed to unity. Individual data points were weighted according to the reciprocal of the variance, as estimated from the frame duration over the total image concentration. A delay, which was fixed over the entire image volume, was estimated by fitting the same spectral analysis model to a time-activity curve (TAC) from regions of interest (ROI) over the entire image volume and varying the delay using a golden line search algorithm to determine the delay that minimised the weighted least squared error.

2.8. Derivation of regional cerebral blood flow

Parametric images of the $H_2{}^{15}O$ kinetic parameter $K1_{H2O}$ ($mL \cdot min^{-1} \cdot ml^{-1}$), a measure of rCBF, were obtained using a one-tissue compartment model in which $K1_{H2O}$ is the rate of uptake of $H_2{}^{15}O$ from blood to brain. An input function of total radioactivity in whole blood was used, which was calculated by scaling the continuous blood data, as with the [^{11}C]-DPN blood data. Reconstructed $H_2{}^{15}O$ PET images were initially smoothed with a 4-mm FWHM Gaussian kernel before kinetic modelling using the Generalized Linear Least Squares (GLLS) algorithm.

2.9. VD_{DPN}, $K1_{DPN}$, and $K1_{H2O}$ image preprocessing

Preprocessing of parametric images was performed using SPM8 (Statistical Parametric Mapping; Wellcome Department of Cognitive Neurology, London, United Kingdom). Each PET image were coregistered onto the corresponding T1-weighted MRI image using rigid body transformation derived from the normalized mutual information measure of image matching.[40] Next, MRI images were spatially normalised into the International Consortium for Brain Mapping (ICBM) standardised space (Montreal Neurological Institute, Montreal, Canada) using nonlinear basis functions, with the same transformation characteristics then applied to the coregistered parametric PET images.

2.10. Calculation of global $K1_{DPN}$

Kinetic modelling of [^{11}C]-DPN using spectral analysis is based on a compartmental model in which delivery of the radiotracer (represented by the parameter $K1_{DPN}$) to brain tissues is modelled separately to specific binding (represented by VD_{DPN}) and nonspecific binding (to other cellular molecules). However, $K1_{DPN}$ would be expected to change along with blood flow as a result of differences in pain state. In particular, delivery effects may act as a confounder of the positive relationship between chronic pain perception and radiotracer binding: it would be expected that chronic pain would increase blood flow to the brain and increase the concentration of radiotracer in regions of interest. We controlled for radiotracer delivery effects within the statistical analysis by removing any variance in VD_{DPN} that could be accounted for by global $K1_{DPN}$ (the parameter estimating radiotracer delivery). Although reliance on global values of $K1_{DPN}$

might not be ideal, we determined that "regional" $K1_{DPN}$ did not correlate with regional VD_{DPN} as a result. The weighted average of $K1_{DPN}$ values in gray matter across the whole brain were therefore calculated for each scan. $K1_{DPN}$ values in gray matter were initially identified using a gray matter mask on $K1_{DPN}$ images.

2.11. Analysis of head motion data

Head motion is a nuisance variable that could potentially cause unwanted between-subject and/or between-group variability in VD_{DPN} values. We therefore controlled for head motion in statistical tests. Quantitative head motion data were collected from the Vicra system, but the raw data were considered unreliable due to the observation that the head was able to move to a small extent within the neoprene cap worn by the participant to mount the head motion sensors. Analysis of head motion data was therefore performed in a semiquantitative manner, in that it relied on some qualitative assessment to achieve an ordinal score of total motion.

Head motion data consisted of both translational and rotational movements, each represented by 3 separate time-courses for each dimension of movement. Using visual inspection of these data, each [^{11}C]-DPN scan was scored separately for (1) intra-scan motion taking place over 2 or more dynamic frames of the PET data, (2) motion taking place between the transmission scan and the [^{11}C]-DPN scan, (3) the magnitude of infrequent intra-frame discrete motion events, and (4) the magnitude of frequent intra-frame motion events (Supplementary Table 2, available online as Supplemental Digital Content at http://links.lww.com/PAIN/A159). Separate scales were used to score each item for the degree of motion observed to account for the likely impact of that motion on the quality of the PET data. Movements of less than 1 mm translation, or 1 degree of rotation (which roughly equates to a 1-mm movement of superficial cortical regions), were considered inconsequential due to the resolution of the PET camera at 2.5 mm. Intraframe motion events were scored higher (and higher again with greater frequency) than motion events spanning across 2 or more dynamic frames of PET data, because the latter were at least partially corrected during reconstruction. Scores for each type of motion were summed to create an overall motion severity score for each scan. Two researchers scored the head motion data independently, and mean values were generated for these scores.

2.12. Assessment of acute thermal pain threshold

The order of PET and thermal pain threshold assessments were randomised between participants and occurred on different days within 4 weeks of each other. Acute pain was induced using a CO_2 laser (150-millisecond duration, beam diameter of 15 mm), which specifically activates nociceptors in the skin,[43] applied to the dorsal surface of the subjects' right forearm. Between stimuli, the laser was moved randomly over an area 3×5 cm to avoid habituation, sensitization, or skin damage, with stimuli occurring at 10-second intervals. Subjects wore protective laser safety goggles.

To determine pain threshold, the Method of Levels was used. Participants were instructed to attend to the intensity of each laser stimulus and to rate it using a 0 to 10 numerical rating scale (NRS), which was anchored such that a level 4 indicated pain threshold, 7 indicated moderate pain, and 10 indicated unbearable pain. Laser stimuli were gradually increased in steps of 0.3 $W{\cdot}cm^{-2}$ stimulus irradiance, from 0 up to a subjective intensity of 7 of 10, and were repeated 3 times. Pain threshold was considered as the mean stimulus energy, over the first 3 ramps, required to elicit a response of 4 of 10.

2.13. Statistical analyses

Statistical analyses were conducted on [^{11}C]-DPN VD images on a voxel-by-voxel basis across the whole brain using SPM8 software. Before whole-brain analyses, smoothing of images was performed using a 3-dimensional Gaussian kernel of 8 mm.

Whole-brain regression analyses were conducted within the patient group (n = 17) to identify regions correlating with sensory and affective dimensions of pain (Short-Form McGill Pain Questionnaire, sensory and affective subscales). In all tests, a number of covariates controlled for nuisance variables: subject age (years), subject sex (binary), subject weight (kg), [^{11}C]-DPN dose injected (MBq), global $K1_{DPN}$ (min^{-1}), head motion scores, and mean NRS ratings of pain reported across the whole scan. For all whole-brain comparisons, results are reported at uncorrected probability thresholds of $P < 0.001$ with a minimum cluster size of 50 voxels, and results are considered statistically significant after voxel-level correction for multiple comparisons using the familywise error rate set to 0.05.

Further analyses were conducted on ROIs whose values were obtained as follows. From each scan, VD_{DPN} values were extracted from ROIs in which suprathreshold clusters (after familywise error correction) were found. Most ROIs were defined by anatomical labels within a previously published probabilistic atlas of the human brain,[26] except for the periaqueductal gray (PAG) whose ROI was constructed from 3 overlapping 6-mm spheres along the central aqueduct (in mm, 0 −24 −4; 0 −26 −6; 0 −29 −8) as done in previous work.[48] A weighted average of VD_{DPN} values within ROIs was calculated. $K1_{DPN}$ and $K1_{H2O}$ values were obtained from ROIs in the same way.

Region of interest analyses sought to identify group differences and correlations with pain threshold. Firstly, ROIs from the patient (n = 17) and healthy control (n = 9) groups were statistically compared using an independent-sample *t* test with significance threshold of $P < 0.05$, after corrections had been made to the mean VD_{DPN} within each ROI by controlling for variance related to nuisance variables. The same nuisance variables were used as in the whole-brain analysis described above. Secondly, ROI data from each group separately, and also from the pooled data across both groups, were correlated with pain threshold as assessed by the acute laser stimuli. Mean ROI values were first corrected for nuisance variables as described above, with an additional variable being each subjects' 0 to 10 NRS rating of acute laser pain intensity. Pearson's product–moment correlation coefficient was obtained, and results were considered statistically significant at $P < 0.05$.

To test whether rCBF explained any of the variances in the VD_{DPN} data after correction for $K1_{DPN}$, mean $K1_{H2O}$ within ROIs were tested for correlation with both mean VD_{DPN} within the same ROIs, and predictor variables of interest showing statistically significant relationships with VD_{DPN} (namely, McGill sensory and affective pain scores and acute pain threshold). $K1_{H2O}$ for the patient (n = 14) and control (n = 8) groups were also compared by independent-sample *t* test in the same way as for the VD_{DPN} data.

3. Results

3.1. Participant characteristics and group comparisons

Data for group comparisons of sex, age, weight, radiotracer doses, intrascan pain ratings, head motion during scanning, and

acute laser thermal pain thresholds are shown in **Table 1**. There was a larger proportion of females in the patient group (that was not statistically significant), and patients were significantly older than healthy controls. The dose of [^{11}C]-DPN injected, and the weight of participants (which may impact on radiotracer concentrations reaching the brain), did not significantly differ between groups, whereas the dose of water injected to assess rCBF was overall greater in patients than controls. On average, patients reported being in greater pain than controls during scanning, but the results were not statistically significant suggesting that efforts to make patients comfortable were at least partially successful. However, patients on average showed more than twice as much head motion during scanning, although this did not reach statistical significance compared with the healthy group. Finally, while patients may scale pain differently because of their previous experience of chronic pain, we found no evidence of a difference in pain thresholds between groups.

3.2. Effect of chronic pain perception on opioid receptor availability

Whole-brain SPM regression analysis (**Figures 1A and B**, Supplementary Table 3, available online as Supplemental Digital Content at http://links.lww.com/PAIN/A159) revealed that in patients with chronic pain, McGill sensory pain scores, for their chronic pain over the previous week, was significantly and positively correlated with OpR availability at the cluster level in the caudate nucleus, continuous with the nucleus accumbens and the subcallosal area. The right mid-insula showed the same effect at just below the level of significance. As the data were corrected for head motion in this statistical model, the greater VD values could not be ascribed to this factor. Also, having corrected for delivery effects in the analysis using the kinetic parameter K1, the mean VD values were not correlated with rCBF in the caudate ($r = 0.27$, $P = 0.35$) nor was rCBF related to chronic pain perception (**Table 2**), suggesting that the relationship between chronic pain perception and VD in the region of interest was not driven by greater blood flow in patients experiencing greater chronic pain.

As confirmation that the main result in the caudate was not related to modification of the endogenous opioid system by recent use of opioid medication, ROI analysis on the whole caudate was found to be comparable for the whole patient group (n = 17, $r = 0.691$, $P = 0.002$) and for a restricted patient group that excluded those withdrawn from opioid medication for the purpose of scanning (n = 15, $r = 0.687$, $P = 0.005$).

Analysis on further ROIs (putamen, insula, thalamus, and PAG, **Table 2**), in which mean VD values were taken over each ROI bilaterally, also revealed significant associations between chronic pain perception and OpR availability, suggesting a broad relationship between chronic pain and OpR availability across a network of brain regions expressing OpRs, including those involved with descending inhibition of nociception. Testing the same ROIs against patients' affective pain perception (McGill affective pain scores) yielded a significant positive relationship within the caudate nucleus and subcallosal area only.

3.3. Opioid receptor availability correlation with pain threshold

Opioid receptor availability was found positively correlate with laser heat pain threshold in both the caudate and subcallosal area (**Table 2**), with the strongest effect in the caudate (**Figure 1C**).

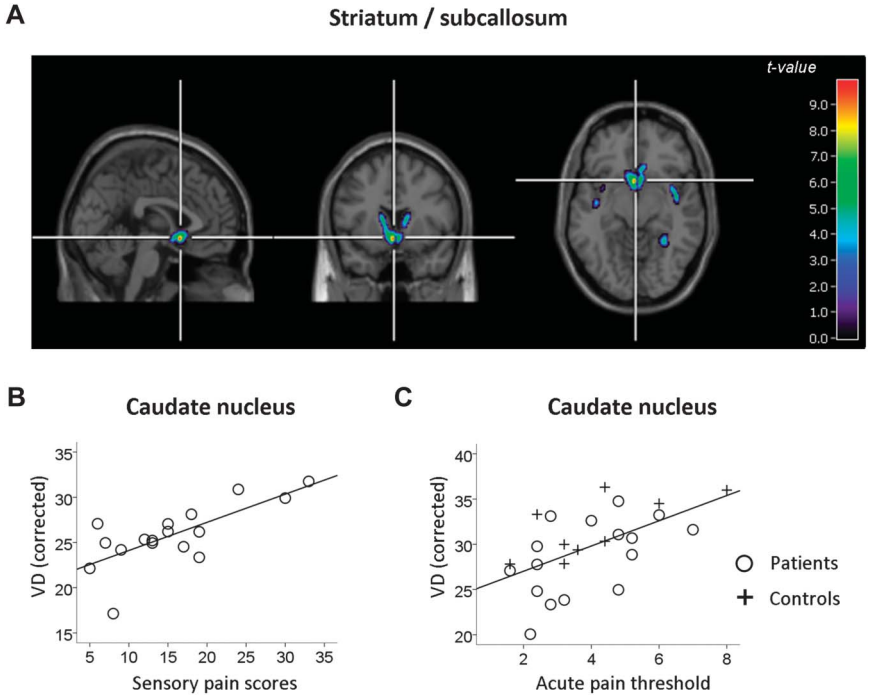

Figure 1. Relationship of ^{11}C-DPN binding to chronic pain perception and acute pain thresholds. The VD, as a proxy of ^{11}C-DPN binding, was adjusted for a number of nuisance variables in each analysis (see Methods). (A) Whole-brain SPM regression analysis of McGill sensory pain scores as a predictor of ^{11}C-DPN binding (patients only, n = 17). Images are displayed at a voxel threshold of $P < 0.001$ uncorrected and a cluster threshold equating to the size of the significant cluster. (B) For illustrative purposes, subsequent extraction of mean VD values from the caudate nucleus was corrected for the same nuisance variables and plotted against McGill sensory pain scores. (C) Pain threshold (laser energy in W·cm^{-2} required to elicit the lowest pain sensation) regressed on VD values (mean across all voxels in the caudate ROI) after correction for nuisance variables. Regression line illustrates fits for the pooled data across groups (patients and controls, n = 26). ROI, region of interest; VD, volume of distribution.

Table 2

Statistics relating to random and fixed effect analyses on ROIs.

	McGill sensory pain		McGill affective pain		Acute pain threshold						Group	
	Arthritis patients		Arthritis patients		Groups pooled		Arthritis patients		Healthy controls		Patients vs controls	
	r	*P*	*r*	*P*	*r*	*P*	*r*	*P*	*r*	*P*	*t*	*P*
Diprenorphine data												
n	17		17		26		17		9		17, 9	
Caud	0.691	*0.002*	0.587	*0.013*	0.596	*0.002*	0.572	*0.021*	0.735	*0.024*	−2.107	*0.047*
Subcal	0.779	*0.001*	0.536	*0.026*	0.424	*0.035*	0.49	0.054	0.339	0.373	−1.728	0.098
NuAcc	0.691	*0.002*	0.356	0.160	0.300	0.146	0.431	0.096	0.044	0.911	−1.452	0.160
Ins	0.653	*0.003*	0.284	0.269	0.377	0.063	0.454	0.077	0.247	0.521	−1.648	0.113
Puta	0.567	*0.018*	0.197	0.449	0.382	0.060	0.476	0.063	0.204	0.598	−1.770	0.090
Thal	0.601	*0.011*	0.346	0.174	0.301	0.144	0.244	0.363	0.427	0.252	−1.258	0.221
ACC	0.454	0.067	−0.029	0.912	0.135	0.520	0.397	0.128	0.343	0.193	−0.976	0.339
PAG	0.561	*0.019*	−0.030	0.910	0.136	0.516	0.075	0.783	0.275	0.474	−0.445	0.660
Water data												
n	14		14		22		14		8		14, 8	
Caud	0.282	0.329	0.208	0.475	0.524	0.012	0.314	0.274	0.701	0.053	−1.013	0.339

Significant effects are italicised.

ACC, anterior cingulate cortex; Caud, caudate nucleus; Ins, insula; NuAcc, nucleus Accumbens; *P*, probability of incorrectly rejecting the null hypothesis; PAG, periaqueductal gray; Puta, putamen; *r*, Pearson's product moment correlation coefficient; Subcal, subcallosal area; Thal, thalamus.

Effects were close to significance in the putamen and insula but not in nucleus accumbens. The strength of the effect was also greater (for caudate and the subcallosal area) in the pooled data over both groups, with individual groups showing weaker relationships (leading to effects above the threshold of significance in the subcallosal area) consistent with the fewer degrees of freedom when considering individual groups.

Pain thresholds were also related to rCBF in the caudate nucleus, but on further assessment rCBF was not related to diprenorphine VD values in the caudate ($r = 0.21$, $P = 0.36$), and so the relationship between OpR binding and rCBF results remains obscure.

3.4. Group differences in opioid receptor availability

Group comparison of mean VD values in ROIs revealed overall lower OpR availability in the caudate nucleus in patients relative to controls (**Table 2**). Although OpR availability was also lower in patients in the subcallosal area and nucleus accumbens, these effects did not reach significance. There were no group differences in any other ROIs, suggesting that these results are specific to the ventral striatum. There were no group differences in rCBF in the caudate nucleus.

4. Discussion

Three key findings emerge from this study: Firstly, the perception of higher levels of chronic pain within the arthritis group was related to greater OpR availability across pain-modulatory regions of the basal ganglia, insula, and PAG, and particularly strongly within the caudate, nucleus accumbens, and subcallosal area. This is the first time this has been reported in patients with arthritic pain. The result is consistent with the hypothesis of upregulation of receptor sites in those experiencing greater chronic pain, although the hypothesis itself is not directly tested here. Secondly, OpR availability in the caudate was positively associated with acute thermal pain threshold (in both patients and controls), supporting the view that upregulation of OpRs in the striatum is adaptive in acting to dampen pain perception. Thirdly, overall caudate OpR availability was reduced in patients with arthritis relative to healthy controls, consistent with greater release of endogenous opioid peptides and consequent occupation of OpR-binding sites in the arthritis group. Our analyses were strengthened by controlling for radiotracer delivery effects and head motion, 2 factors that are likely to be both responsive to pain states and have an influence on PET radioligand results.

4.1. OpR availability in chronic pain

The positive relationship between OpR availability and recent chronic pain perception could result either from a greater density of OpRs on neuronal cellular membranes (eg, due to increased trafficking or upregulation), reduced opioid "tone" (reduced release of endogenous opioid peptides resulting in reduced occupation of OpRs), or both. With single scans, it is not possible to directly measure opioid tone and OpR density independently. However, opioid "tone" is highly dependent on the current pain state, as illustrated by the fact that induction of acute pain for a short time during PET scanning procedures can be enough to cause a reduction in OpR availability as a result of endogenous opioid release and competitive binding to OpRs.[54] Yet, our data showing a positive association between OpR availability and previous chronic pain perception was statistically independent of intrascan pain perception. This does not favour the explanation that variability in the concentration of endogenous opioid peptides, released due to intrascan pain, were causing the positive correlation between OpR availability and previous chronic pain state.

Our analysis shows that the variances in OpR availability in the caudate nucleus explained by acute pain threshold were present in both patients with chronic pain and healthy controls. These variances can therefore be explained by natural variability in OpR density that is independent of the presence of arthritic disease and chronic pain symptoms. A greater density of OpRs would be expected to increase the sensitivity of postsynaptic neurons to opioid-mediated inhibition in response to pain, thereby increasing "gain" in the system.

In animals, delta- and kappa-OpRs in the brain and spinal cord were upregulated in response to mu-OpR agonism.[8,11,56] For mu-OpRs, there is only evidence of upregulation in

response to "reduced" neurotransmitter binding, just as the normal adaptation to "greater" binding (eg, in response to morphine[59]) is receptor downregulation. This may account for the greater antinociceptive effects of delta-selective agonists than nonselective agonists in chronic pain states. Together, this evidence implies that delta- and kappa-OpR upregulation would be an expected consequence of chronic pain states. Given that [^{11}C]-DPN is nonselective to OpR subtypes, detection of such an upregulatory response is facilitated and may explain why studies using mu-selective ligands[28] have not detected this mechanism.

Bringing this together, the most likely explanation for our findings is that there is an adaptive upregulation of OpRs in response to chronic pain and that in general greater OpR binding is associated with higher pain threshold and therefore greater pain resilience.

4.2. Group differences

The finding of overall lower OpR availability in patients vs controls may be a result of competition for OpR binding by the release of endogenous ligands as a result of pain being experienced during scanning, and possibly the recycling of receptors as a direct result of this. This finding is consistent with previous studies; reduced OpR availability in the human brain has been associated with RA,[30] peripheral neuropathic pain,[32,39] and fibromyalgia.[28] However, considering these earlier studies, it is surprising that we did not find group differences across more widespread brain regions, with results being restricted to the striatum. It is possible that our study is underpowered to detect differences between groups there are poorly balanced for age and sex. However, patients in our study were also made as comfortable as possible during scanning. The activity-dependent nature of pain in many patients with OA may mean that patients were able to achieve a greater level of comfort inside the scanner that has been possible in patients from these previous studies whose pain is likely to persist when at rest. As shown in **Table 1**, although a small number of patients did experience some discomfort that led to higher mean and variance in intrascan pain scores in the patient group relative to controls, the ratings are still within the nonpainful range.

However, it has been unclear whether findings of lower OpR availability in patients with chronic pain compared with pain-free control subjects reflect greater vulnerability to chronic pain states (ie, reduced OpR density resulting in reduced ability to dampen pain perception through opioidergic inhibition) or are merely a consequence of greater synaptic concentrations of endogenous opioids, released in response to pathological nociception, that compete with the same binding sites as opioid radiotracers. Our findings suggesting upregulation of OpRs in response to chronic arthritic pain clarify that the latter explanation for reductions in OpR availability in chronic pain states is the most likely and that there is increased release of endogenous opioid peptides in chronic arthritic pain.

4.3. Striatal mechanisms in chronic pain perception

The striatal dopamine and opioid systems have previously been shown to be abnormal in chronic pain syndromes. Patients with fibromyalgia and orofacial pain syndromes[24,25] have an abnormal dopamine response to pain in the caudate and putamen.[57] Furthermore, there is evidence of increased gray matter density in the striatum in a number of chronic pain conditions including fibromyalgia,[50] chronic low back pain,[49] and chronic vulvar pain.[51] It is not yet clear how these abnormalities relate to the endogenous opioid system or to pain perception.

Abnormalities in both dopaminergic and opioidergic neurotransmission in the striatum in patients with chronic pain might reflect motivational and motor processes such as the learning or expression of conditioned responses to pain.[16] The ventral striatum is a region commonly associated with signalling rewarding outcomes and mediating reinforcement of appetitive behaviour. However, it is also commonly activated during anticipation of pain stimuli,[17] particularly the caudate nucleus.[47] Pavlovian prediction learning and evaluation has been associated with the "limbic loop," including the ventral striatum, the basolateral amygdala, and the orbitofrontal cortex.[10,29] The nucleus accumbens, in particular, brings evaluative information from the orbitofrontal cortex and amygdala to bear on performance by selectively gating information projecting to basal ganglia output nuclei.[2,23] The above networks are involved with the generation of prediction errors for rewarding and aversive stimuli.[46,53] However, prediction error signals in the nucleus accumbens have been specifically associated with Pavlovian conditioning, whereas prediction errors required for instrumental conditioning involve the putamen.[45]

There is also evidence for a relationship between dopamine receptor binding in the ventral striatum (nucleus accumbens) with affective responses to pain.[52] Ventral striatal reward mechanisms may therefore be directly implicated in driving the affective component of pain. However, our data showing a stronger correlation of OpR availability with the sensory than the affective components of pain cast doubt on this hypothesis and suggest that the ventral striatum may have a more general motivational function in driving behavioural responses to pain. This is consistent with previous work demonstrating that stimulation of the caudate in monkey reduces behavioural reactivity to acute pain.[37]

5. Conclusions

Our data are consistent with an upregulation of OpRs in response to chronic pain in humans, a hypothesis first identified from animal research and suggested to be part of a homeostatic mechanism that dampens pain perception. This is the first observational evidence consistent with this hypothesis in humans, supported by a correlation between OpR availability and pain resilience (greater pain threshold) in the caudate nucleus. Longitudinal studies are required to identify whether failure to adequately upregulate OpRs in response to chronic pain may be a risk factor for a more extreme and/or refractory phenotype. Further sequential studies are needed to examine the benefits and pitfalls of current therapeutic approaches to chronic pain in terms of their effects on OpR availability in the brain and the potential for increasing resilience to developing chronic pain from the outset.

Conflict of interest statement

The authors have no conflicts of interest to declare.

The study was funded by a project grant from the Medical Research Council (Grant Reference G0800522) in the United Kingdom.

Acknowledgements

We extend our gratitude to all staff at the Wolfson Molecular Imagine Centre who were essential for the success of this project,

in particular Professor Karl Herholz and Dr Peter Talbot who helped with the initial concept and design, and the radiographers, radiochemists, and blood laboratory for helping to implement the study. We also wish to thank the consultant anaesthetists who aided in the collection of blood data, and a special thanks to our research nurse Ann Lenton who was crucial for patient recruitment.

Appendix A. Supplemental Digital Content

Supplemental Digital Content associated with this article can be found online at http://links.lww.com/PAIN/A159.

Article history:
Received 19 February 2015
Received in revised form 18 June 2015
Accepted 6 July 2015
Available online 14 July 2015

References

[1] Aletaha D, Neogi T, Silman AJ, Funovits J, Felson DT, Bingham CO, Birnbaum NS, Burmester GR, Bykerk VP, Cohen MD, Combe B, Costenbader KH, Dougados M, Emery P, Ferraccioli G, Hazes JMW, Hobbs K, Huizinga TWJ, Kavanaugh A, Kay J, Kvien TK, Laing T, Mease P, Ménard HA, Moreland LW, Naden RL, Pincus T, Smolen JS, Stanislawska-Biernat E, Symmons D, Tak PP, Upchurch KS, Vencovský J, Wolfe F, Hawker G. 2010 rheumatoid arthritis classification criteria: an American college of rheumatology/European league against rheumatism collaborative initiative. Arthritis Rheum 2010;62:2569–81.

[2] Alheid GF, Heimer L. New perspectives in basal forebrain organization of special relevance for neuropsychiatric disorders: the striatopallidal, amygdaloid, and corticopetal components of substantia innominata. Neuroscience 1988;27:1–39.

[3] Altman R, Alarcón G, Appelrouth D, Bloch D, Borenstein D, Brandt K, Brown C, Cooke TD, Daniel W, Feldman D, Greenwald R, Hochberg M, Howell D, Ike R, Kapila P, Kaplan D, Koopman W, Marino C, McDonald E, McShane DJ, Medsger T, Michel B, Murphy WA, Osial T, Ramsey-Goldman R, Rothschild B, Wolfe F. The American college of rheumatology criteria for the classification and reporting of osteoarthritis of the hip. Arthritis Rheum 1991;34:505–14.

[4] Baumgärtner U, Buchholz H-GG, Bellosevich A, Magerl W, Siessmeier T, Rolke R, Höhnemann S, Piel M, Rösch F, Wester H-JJ, Henriksen G, Stoeter P, Bartenstein P, Treede R-DD, Schreckenberger M, Baumgartner U, Hohnemann S, Rosch F. High opiate receptor binding potential in the human lateral pain system. Neuroimage 2006;30:692–9.

[5] Bedson J, Croft PR. The discordance between clinical and radiographic knee osteoarthritis: a systematic search and summary of the literature. BMC Musculoskelet Disord 2008;9:116–26.

[6] Braz JM, Nassar MA, Wood JN, Basbaum AI. Parallel "pain" pathways arise from subpopulations of primary afferent nociceptor. Neuron 2005; 47:787–93.

[7] Cahill CM, Holdridge SV, Morinville A. Trafficking of delta-opioid receptors and other G-protein-coupled receptors: implications for pain and analgesia. Trends Pharmacol Sci 2007;28:23–31.

[8] Cahill CM, McClellan KA, Morinville A, Hoffert C, Hubatsch D, O'Donnell D, Beaudet A. Immunohistochemical distribution of delta opioid receptors in the rat central nervous system: evidence for somatodendritic labeling and antigen-specific cellular compartmentalization. J Comp Neurol 2001; 440:65–84.

[9] Cahill CM, Morinville A, Hoffert C, Donnell DO, Beaudet A. Up-regulation and trafficking of d opioid receptor in a model of chronic inflammation: implications for pain control. PAIN 2003;101:199–208.

[10] Cardinal RN, Parkinson JA, Hall J, Everitt BJ. Emotion and motivation: the role of the amygdala, ventral striatum, and prefrontal cortex. Neurosci Biobehav Rev 2002;26:321–52.

[11] Cheng PY, Svingos AL, Wang H, Clarke CL, Jenab S, Beczkowska IW, Inturrisi CE, Pickel VM. Ultrastructural immunolabeling shows prominent presynaptic vesicular localization of delta-opioid receptor within both enkephalin- and nonenkephalin-containing axon terminals in the superficial layers of the rat cervical spinal cord. J Neurosci 1995;15: 5976–88.

[12] Chudler EH, Dong WK. The role of the basal ganglia in nociception and pain. PAIN 1995;60:3–38.

[13] Comtat C, Sureau FC, Sibomana M, Hong IK, Sjoholm N, Trebossen R. Image based resolution modeling for the HRRT OSEM reconstructions software. 2008 IEEE Nuclear Science Symposium Conference Record. IEEE, 2008. pp. 4120–3. doi:10.1109/NSSMIC.2008.4774188.

[14] Cross AJ, Hille C, Slater P. Subtraction autoradiography of opiate receptor subtypes in human brain. Brain Res 1987;418:343–8.

[15] Cunningham VJ, Jones T. Spectral analysis of dynamic PET studies. J Cereb Blood Flow Metab 1993;13:15–23.

[16] Daw ND, Shohamy D. The cognitive neuroscience of motivation and learning. Soc Cogn 2008;26:593–620.

[17] Delgado MR, Li J, Schiller D, Phelps EA. The role of the striatum in aversive learning and aversive prediction errors. Philos Trans R Soc Lond B Biol Sci 2008;363:3787–800.

[18] Fairclough M, Prenant C, Brown G, McMahon A, Lowe J, Jones A. The automated radiosynthesis and purification of the opioid receptor antagonist, [6-O-methyl-(11) C]diprenorphine on the GE TRACERlab FXFE radiochemistry module. J Labelled Comp Radiopharm 2014;57: 388–96.

[19] Fields H. State-dependent opioid control of pain. Nat Rev Neurosci 2004; 5:565–75.

[20] Garcia-Larrea L, Peyron R. Pain matrices and neuropathic pain matrices: a review. PAIN 2013;154:S29–43.

[21] Gear RW, Aley KO, Levine JD. Pain-induced analgesia mediated by mesolimbic reward circuits. J Neurosci 1999;19:7175–81.

[22] Gendron L, Lucido AL, Mennicken F, O'Donnell D, Vincent JP, Stroh T, Beaudet A. Morphine and pain-related stimuli enhance cell surface availability of somatic delta-opioid receptors in rat dorsal root ganglia. J Neurosci 2006;26:953–62.

[23] Groenewegen HJ, Wright CI, Beijer A V, Voorn P. Convergence and segregation of ventral striatal inputs and outputs. Ann N Y Acad Sci 1999; 877:49–63.

[24] Hagelberg N, Forssell H, Aalto S, Rinne JO, Scheinin H, Taiminen T, Någren K, Eskola O, Jääskeläinen SK. Altered dopamine D2 receptor binding in atypical facial pain. PAIN 2003;106:43–8.

[25] Hagelberg N, Forssell H, Rinne JO, Scheinin H, Taiminen T, Aalto S, Luutonen S, Nagren K, Jaaskelainen S. Striatal dopamine D1 and D2 receptors in burning mouth syndrome. PAIN 2003;101:149–54.

[26] Hammers A, Allom R, Koepp MJ, Free SL, Myers R, Lemieux L, Mitchell TN, Brooks DJ, Duncan JS. Three-dimensional maximum probability atlas of the human brain, with particular reference to the temporal lobe. Hum Brain Mapp 2003;19:224–47.

[27] Hammers A, Asselin MC, Turkheimer FE, Hinz R, Osman S, Hotton G, Brooks DJ, Duncan JS, Koepp MJ. Balancing bias, reliability, noise properties and the need for parametric maps in quantitative ligand PET: [(11)C]diprenorphine test-retest data. Neuroimage 2007;38: 82–94.

[28] Harris RE, Clauw DJ, Scott DJ, McLean SA, Gracely RH, Zubieta JK. Decreased central mu-opioid receptor availability in fibromyalgia. J. Neurosci 2007;27:10000–6.

[29] Holland P, Gallagher M. Amygdala circuitry in attentional and representational processes. Trends Cogn Sci 1999;3:65–73.

[30] Jones AK, Cunningham VJ, Ha-Kawa S, Fujiwara T, Luthra SK, Silva S, Derbyshire S, Jones T. Changes in central opioid receptor binding in relation to inflammation and pain in patients with rheumatoid arthritis. Br J Rheumatol 1994;33:909–16.

[31] Jones AK, Friston K, Dolan R. Positron emission tomography as a research tool in the investigation of psychiatric and psychological disorders. Baillieres Clin Endocrinol Metab 1991;5:187–203.

[32] Jones AK, Kitchen ND, Watabe H, Cunningham VJ, Jones T, Luthra SK, Thomas DG. Measurement of changes in opioid receptor binding in vivo during trigeminal neuralgic pain using [11C] diprenorphine and positron emission tomography. J Cereb Blood Flow Metab 1999;19:803–8.

[33] Jones AK, Luthra SK, Pike VW, Herold S, Brady F. New labelled ligand for in-vivo studies of opioid physiology. Lancet 1985;2:665–6.

[34] Jones AK, Qi LY, Fujirawa T, Luthra SK, Ashburner J, Bloomfield P, Cunningham VJ, Itoh M, Fukuda H, Jones T. In vivo distribution of opioid receptors in man in relation to the cortical projections of the medial and lateral pain systems measured with positron emission tomography. Neurosci Lett 1991;126:25–8.

[35] De Jong HWAM, van Velden FHP, Kloet RW, Buijs FL, Boellaard R, Lammertsma AA. Performance evaluation of the ECAT HRRT: an LSO-LYSO double layer high resolution, high sensitivity scanner. Phys Med Biol 2007;52:1505–26.

[36] Knoess C, Rist J, Michel C, Burbar Z, Eriksson L, Panin V, Byars L, Lenox M, Wienhard K, Heiss W-D, Nutt R. Evaluation of single photon transmission for the HRRT. 2003 IEEE Nuclear Science Symposium. Conference Record (IEEE Cat. No.03CH37515). IEEE 2003;3:1936–40. doi:10.1109/NSSMIC.2003.1352258.
[37] Lineberry CG, Vierck CJ. Attenuation of pain reactivity by caudate nucleus stimulation in monkeys. Brain Res 1975;98:119–34.
[38] Ma J, Zhang Y, Kalyuzhny AE, Pan ZZ. Emergence of functional delta-opioid receptors induced by long-term treatment with morphine. Mol Pharmacol 2006;69:1137–45.
[39] Maarrawi J, Peyron R, Mertens P, Costes N, Magnin M, Sindou M, Laurent B, Garcia-Larrea L. Differential brain opioid receptor availability in central and peripheral neuropathic pain. PAIN 2007;127:183–94.
[40] Maes F, Collignon A, Vandermeulen D, Marchal G, Suetens P. Multimodality image registration by maximization of mutual information. IEEE Trans Med Imaging 1997;16:187–98.
[41] Martikainen IK, Peciña M, Love TM, Nuechterlein EB, Cummiford CM, Green CR, Harris RE, Stohler CS, Zubieta J-K. Alterations in endogenous opioid functional measures in chronic back pain. J Neurosci 2013;33:14729–37.
[42] Melzack R. The short-form McGill pain questionnaire. PAIN 1987;30: 191–7.
[43] Meyer RA, Walker RE, Mountcastle VB Jr. A laser stimulator for the study of cutaneous thermal and pain sensations. IEEE Trans Biomed Eng 1976; 23:54–60.
[44] Morinville A, Cahill CM, Esdaile MJ, Aibak H, Collier B, Kieffer BL, Beaudet A. Regulation of delta-opioid receptor trafficking via mu-opioid receptor stimulation: evidence from mu-opioid receptor knock-out mice. J Neurosci 2003;23:4888–98.
[45] O'Doherty J, Dayan P, Schultz J, Deichmann R, Friston K, Dolan RJ. Dissociable roles of ventral and dorsal striatum in instrumental conditioning. Science 2004;304:452–4.
[46] O'Doherty JP, Dayan P, Friston K, Critchley H, Dolan RJ. Temporal difference models and reward-related learning in the human brain. Neuron 2003;38:329–37.
[47] Palermo S, Benedetti F, Costa T, Amanzio M. Pain anticipation: an activation likelihood estimation meta-analysis of brain imaging studies. Hum Brain Mapp 2015;36:1648–61.
[48] Roy M, Shohamy D, Daw N, Jepma M, Wimmer GE, Wager TD. Representation of aversive prediction errors in the human periaqueductal gray. Nat Neurosci 2014;17:1607–12.
[49] Schmidt-Wilcke T, Leinisch E, Gänßbauer S, Draganski B, Bogdahn U, Altmeppen J, May A. Affective components and intensity of pain correlate with structural differences in gray matter in chronic back pain patients. PAIN 2006;125:89–97.
[50] Schmidt-Wilcke T, Luerding R, Weigand T, Jürgens T, Schuierer G, Leinisch E, Bogdahn U. Striatal grey matter increase in patients suffering from fibromyalgia—a voxel-based morphometry study. PAIN 2007;132: S109–16.
[51] Schweinhardt P, Kuchinad A, Pukall CF, Bushnell MC. Increased gray matter density in young women with chronic vulvar pain. PAIN 2008;140: 411–19.
[52] Scott DJ, Heitzeg MM, Koeppe RA, Stohler CS, Zubieta J-K. Variations in the human pain stress experience mediated by ventral and dorsal basal ganglia dopamine activity. J Neurosci 2006;26:10789–95.
[53] Seymour B, Doherty JPO, Dayan P, Koltzenburg M, Jones AK, Dolan RJ, Friston KJ, Frackowiak RS, O'Doherty JP. Temporal difference models describe higher-order learning in humans. Nature 2004;429: 664–7.
[54] Sprenger T, Valet M, Boecker H, Henriksen G, Spilker ME, Willoch F, Wagner KJ, Wester HJ, To TR, Tolle TR. Opioidergic activation in the medial pain system after heat pain. PAIN 2006;122:63–7.
[55] Tadokoro M, Jones AKP, Cunningham VJ, Sashin D, Grootoonk S, Ashburner J, Jones T. Parametric images of [11C]diprenorphine binding using spectral analysis of dynamic PET images acquired in 3D. Ann Nucl Med 1993;7:S50–51.
[56] Wang XM, Zhou Y, Spangler R, Ho A, Han JS, Kreek MJ. Acute intermittent morphine increases preprodynorphin and kappa opioid receptor mRNA levels in the rat brain. Mol Brain Res 1999;66:184–7.
[57] Wood PB, Schweinhardt P, Jaeger E, Dagher A, Hakyemez H, Rabiner EA, Bushnell MC, Chizh BA. Fibromyalgia patients show an abnormal dopamine response to pain. Eur J Neurosci 2007;25:3576–82.
[58] Woolf AD, Pfleger B. Burden of major musculoskeletal conditions. Bull World Health Organ 2003;81:646–56.
[59] Zadina JE, Chang SL, Ge LJ, Kastin AJ. Mu opiate receptor down-regulation by morphine and up-regulation by naloxone in SH-SY5Y human neuroblastoma cells. J Pharmacol Exp Ther 1993;265: 254–62.
[60] Zubieta J, Smith YR, Bueller JA, Xu Y, Kilbourn MR, Jewett DM, Meyer CR, Koeppe RA, Stohler CS. Regional mu opioid receptor regulation of sensory and affective dimensions of pain. Science 2001;293:311–5.